Cellular Oncology
https://doi.org/10.1007/s13402-022-00660-1

SHORT COMMUNICATION

PKP1 and MYC create a feedforward loop linking transcription and translation in squamous cell lung cancer

Laura Boyero[1,2,3] · Joel Martin-Padron[1,2] · María Esther Fárez-Vidal[2,4] · Maria Isabel Rodriguez[1,2,4] · Álvaro Andrades[1,4,5] · Paola Peinado[1,3,5] · Alberto M. Arenas[1,5] · Félix Ritoré-Salazar[1,5] · Juan Carlos Alvarez-Perez[1,4,5] · Marta Cuadros[1,2,4] · Pedro P. Medina[1,4,5]

Accepted: 12 January 2022

Abstract

Purpose Plakophilin 1 (PKP1) is well-known as an important component of the desmosome, a cell structure specialized in spot-like cell-to-cell adhesion. Although desmosomes have generally been associated with tumor suppressor functions, we recently found that PKP1 is recurrently overexpressed in squamous cell lung cancer (SqCLC) to exert an oncogenic role by enhancing the translation of MYC (c-Myc), a major oncogene. In this study, we aim to further characterize the functional relationship between PKP1 and MYC.

Methods To determine the functional relationship between PKP1 and MYC, we performed correlation analyses between *PKP1* and *MYC* mRNA expression levels, gain/loss of function models, chromatin immunoprecipitation (ChIP) and promoter mutagenesis followed by luciferase assays.

Results We found a significant correlation between the mRNA levels of *MYC* and *PKP1* in SqCLC primary tumor samples. In addition, we found that MYC is a direct transcription factor of PKP1 and binds to specific sequences within its promoter. In agreement with this, we found that MYC knockdown reduced PKP1 protein expression in different SqCLC models, which may explain the PKP1-MYC correlation that we found. Conversely, we found that PKP1 knockdown reduced MYC protein expression, while PKP1 overexpression enhanced MYC expression in these models.

Conclusions Based on these results, we propose a feedforward functional relationship in which PKP1 enhances MYC translation in conjunction with the translation initiation complex by binding to the 5'-UTR of *MYC* mRNA, whereas MYC promotes *PKP1* transcription by binding to its promoter. These results suggest that PKP1 may serve as a therapeutic target for SqCLC.

Keywords Non-small cell lung cancer · Squamous cell lung cancer · Plakophilin · MYC · Biomarker · Feedforward loop

1 Introduction

Currently, lung cancer is the cancer with the highest mortality rate world-wide, being responsible for ~ 25% of cancer associated deaths [1]. Despite the relevant immunotherapeutic breakthroughs that have been made based on immune checkpoint inhibitors, more than 80% of patients with non-small cell lung cancer (NSCLC) find it difficult to benefit from them [2, 3], mainly due to immune evasion [4]. Therefore, there is still a need to develop novel more effective therapies.

The *plakophilin-1* (*PKP1*) gene encodes a member of the armadillo catenin family and the plakophilin subfamily. Plakophilins are important components of the desmosome, a cell structure specialized in spot-like cell-to-cell adhesion that strengthens the bonds between cells in the supra-basal

✉ Pedro P. Medina
pedromedina@ugr.es

1 Pfizer-University of Granada-Junta de Andalucía Centre for Genomics and Oncological Research (GENYO), Granada, Spain

2 Department of Biochemistry and Molecular Biology III, University of Granada, Granada, Spain

3 Present Address: Institute of Biomedicine of Seville (IBiS) (HUVR, CSIC, University of Seville), Seville, Spain

4 Institute for Biomedical Research Ibs. Granada, University Hospital Complex of Granada/University of Granada, Granada, Spain

5 Department of Biochemistry and Molecular Biology I, University of Granada, Granada, Spain

Published online: 19 February 2022

layers of epithelia that undergo mechanical stress [5]. In particular, plakophilins are essential components of desmosomal plaques, where they interact with desmosomal cadherins and the cytoskeletal linker protein desmoplakin, thereby stabilizing the desmosomal proteins at the plasma membrane.

Homozygous or compound heterozygous mutations in *PKP1* result in fewer and poorly formed desmosomes and a loss of epidermal integrity causing ectodermal dysplasia-skin fragility syndrome [6], a rare inherited autosomal recessive syndrome of which only 21 cases have been reported in the literature up to 2017 [7]. In cancer, desmosomes have been associated with tumor suppressor functions [8]. However, PKP1 has been reported to rank among the top overexpressed proteins in squamous cell lung cancer (SqCLC) [1, 9, 10] and has been identified as a specific marker of this major subtype of NSCLC [11]. To face this apparent paradox, we recently investigated whether PKP1 may have additional functions beyond its well-known role in desmosomes. We found that PKP1 plays an oncogenic role in SqCLC, promoting cell proliferation and carcinogenesis in both in vivo and in vitro models by enhancing MYC translation [12]. This post-transcriptional regulation of MYC (also known as c-Myc) was found to be brought about by interaction of PKP1 with the poly(A) binding protein (PABP) [12] and other members of the translation initiation complex. This interaction facilitates the unwinding of complex secondary structures present within the 5'UTR region of some mRNAs, such as MYC, thereby increasing ribosomal translation activity [13].

MYC is a transcription factor that plays an evolutionarily conserved role in controlling cell proliferation, growth and protein synthesis. *MYC* ranks among the most studied oncogenes [14] and has been found to regulate the expression of multiple components of the protein synthesis machinery (including ribosomal proteins, translation initiation factors and rDNA) [15]. Therefore, the functional interaction between PKP1 and MYC may have an important impact on cancer development.

Here, we found that the *PKP1* and *MYC* mRNA levels correlate in SqCLC. Since this correlation cannot be explained by our former observation that PKP1 enhances MYC translation without disturbing its mRNA level [12], we performed a more detailed analysis of the functional association between MYC and PKP1. We found that MYC binds to the *PKP1* promoter to enhance its transcription, creating a feedforward loop that links transcription and translation in SqCLC.

2 Materials and methods

2.1 Cell culture

SK-MES-1, H-2170, LUDLU-1, LC-319 and H520 cells were cultured in DMEM medium supplemented with 10% FCS. EPLC-272H cells were cultured in RPMI-1640 medium supplemented with 10% FCS. L-glutamine as well as antibiotics and antimycotic agents were also added to the cell culture media. Cells were grown in monolayers and maintained at 37 °C in an atmosphere of humidified air with 5% CO_2. All cells were obtained from the ATCC collection. Mycoplasma testing was conducted using a Venor GeM-qEP kit from Minerva Biolabs (#11–9250).

2.2 Analyses of lung cancer patient datasets

To assess the correlation between *PKP1* and *MYC* mRNA expression, we downloaded data from datasets GSE18842 and GSE43580 from the Gene Expression Omnibus using the R package GEOquery (R version 4.0.2, package version 2.56.0). For each gene, we averaged the expression values of all of its available probes after which we plotted the log2-transformed mRNA expression values of *PKP1* against *MYC* and *TBP* (as a negative control). Next, we calculated the Pearson correlation coefficients.

2.3 Analyses of TCGA datasets

Transcriptome profiling data from The Cancer Genome Atlas datasets (TCGA) were downloaded using the R package "TCGAbiolinks". mRNA expression data from primary tumors and solid tissue normal samples, as well as copy number data from primary tumors, were retrieved from the following datasets: LUSC (Lung Squamous Carcinoma), LUAD (Lung Adenocarcinoma), CESC (Cervix Squamous Cell Neoplasm), HNSC (Head and Neck Squamous Cancer) and ESCA (Esophageal Carcinoma). Only tumors labeled as "squamous" and normal solid tissue samples were used for the analyses. For copy number analyses, samples that had more than one data point were considered. *MYC* amplification/deletion was considered if at least one of the data points indicated this.

2.4 PKP1 knockdown

4 h before transfection, 2×10^5 – 5×10^5 cells/well were seeded in 6-well plates in appropriate medium. After 24 h, the cells were transfected with 7.5 nM of a combination of two siRNAs to target *PKP1* or one siRNA to target *MYC*, using Lipofectamine RNAiMAX reagent in accordance with the manufacturer's protocol. After 72 h of incubation, the cells were processed for further analysis. The siRNA-PKP1 mix included Catalog #s10580 and Catalog #s10582 of Silencer Select siRNA (Ambion, Catalog #4392420). The siRNA against *MYC* was Catalog #sc-29226 (Santa Cruz Biotechnology). As a control, scrambled siRNA (siSC; Ambion, Catalog #4390843) was used in each experiment (listed in Table 1). Down-regulation of PKP1 or MYC

protein expression was confirmed by quantitative real time-PCR and Western blotting, as described below.

2.5 Exogenous PKP1 expression

Stable PKP1-expressing transfectants were established according to standard protocols. Lentiviral particles were obtained by transient co-transfection of HEK293T cells using LipoD293 (SignaGen, SL100668) according to the manufacturer's instructions. The plasmids were used in a 2:1:3 ratio and included the packaging construct psPAX.2 (Addgene, #12260), a VSV-G plasmid encoding the envelope (Addgene, #8454) and second-generation pLVX-PKP1A-Myc-DDK-IRES-ZsGreen1 [12] or pLVX-IRES-ZsGreen1 empty vector plasmids (Clontech, 632187). Supernatants were harvested 48 and 72 h after transfection, clarified by 0.45-µm filtration, and stored at − 80 °C until use. To obtain stable transfectants, cells at 80% confluence were infected by three transduction cycles in the presence of polybrene (8 mg/ml), analyzed by flow cytometry using a BD FACS-Canto II (BD Biosciences), sorted when appropriate using BD FACSAria (BD bioscience) and next subjected to further experiments.

2.6 Western blotting

Cell lysates were prepared in RIPA buffer (150 mM NaCl, 1% NP-40, 0.5% sodium deoxycholate, 0.1% SDS and 50 mM Tris–HCl pH 7.5) containing protease and phosphatase inhibitors (0.2 mM PMSF, 7 mM OV4 and Complete Mini EDTA-free Protease Inhibitor Cocktail Tablets). Protein concentrations were determined using Bradford reagent (Amresco) with BSA as a standard. 25 µg total protein was subjected to 10% SDS-PAGE. The resolved samples were subsequently transferred to PVDF membranes and blocked for 1 h in PBS containing 5% non-fat dry milk and 0.1% Tween. Next, they were incubated overnight at 4 °C with primary antibodies (anti-PKP1, Sigma, Catalog #HPA027221, 1:250; anti-MYC, Cell Signaling, Catalog #5605, 1:1000; anti-β-actin, Sigma, Catalog #A5441), and then with secondary antibodies (anti-rabbit HRP, Dako, Catalog #P0448, 1:2000 or anti-mouse HRP, Dako, Catalog #P0447, 1:1000) at room temperature for 1 h. For protein detection, we used a chemiluminescence Western blotting analysis system ChemiDoc (BioRad). β-actin was used as internal control. Band quantification was carried out using t he Plot Lanes tool of ImageJ v1.52a software and normalized according the respective β-actin level.

2.7 Quantitative real time-PCR (qRT-PCR)

Total RNA was isolated from cultured cells using Trizol reagent (Gibco) according to the manufacturer's protocol. The RNA concentration and purity for each sample were measured using a Nanodrop 2000c Spectrophotometer (Thermo Fisher Scientific) after which 1 µg RNA was reverse transcribed using random primers and an iScript transcriptase kit (BioRad). The reverse transcription products were amplified using an iTaq Universal SYBR Green Supermix kit (BioRad), following the manufacturer's instructions and an ABI 7500 Real-Time PCR Detection System (Applied Biosystems). All PCR reactions involved initial denaturation at 95ºC for 30 s followed by 40 cycles at 95 °C for 15 s and 60 °C for 60 s. The following primers were used for PCR: PKP1 forward, 5′-TCAGCAACAAGAGCGACAAG-3′; PKP1 reverse, 5′-TCAGGTAGGTGCGGATGG-3′; TBP forward, 5′-CACGCCAGCTTCGGAGAGT-3′, TBP reverse, 5′-GGCACGAAGTGCAATGGTCC-3′ (Sigma). Each experiment was run in triplicate. Gene expression levels were calculated using the $2^{-\Delta\Delta Ct}$ method, and TBP expression was used as a reference value.

2.8 Chromatin immunoprecipitation (ChIP)

ChIP analysis was performed using a ChromaFlash High-Sensitivity ChIP Kit from Epigentek, Farmingdale, NY (cat #P-2027–24) following the manufacturer's protocol. Briefly, 5×10^6 SK-MES-1 cells were subjected to crosslinking by adding cell culture medium containing formaldehyde to a final concentration of 1% and incubation at room temperature (20–25 °C) for 10 min on a rocking platform (50–100 rpm). Glycine (1.25 M) was added (1:10) to stop the crosslinking. After appropriate mixing, ice-cold PBS washing and centrifuging, lysis buffer was added to resuspend the cell pellet, after which the cells were incubated on ice for 10 min. After carefully removing the supernatant, ChIP buffer was added to resuspend the chromatin pellet. Chromatin was sheared using a

Table 1 siRNAs and their sequences

siRNA	Target gene	ID	5'→3' Sense sequence	5'→3' Antisense sequence
siPKP1-1	PKP1	s10580	GGCUGACAAUUACAACUAUtt	AUAGUUGUAAUUGUCAGCCaa
siPKP1-2	PKP1	s10582	GCUUUGCCGUCGGACCAAAtt	UUUGGUCCGACGGCAAAGCca
siMYC	MYC	sc-29226	AACAGAAAUGUCCUGAGCAAU	AUUGCUCAGGACAUUUCUGUU
Scramble (siSC)	-	4390843	UAACGACGCGACGACGUAAtt	UUACGUCGUCGCGUCGUUAtt

Bioruptor® Plus apparatus (Diagenode) with high power mode for 10 cycles (sonication cycle: 30 s ON, 30 s OFF). Next, the samples were centrifuged at 12,000 rpm at 4 °C for 10 min, and the supernatants were transferred to new vials. Anti-MYC or non-immune IgG antibody were added to antibody buffer (provided in the kit) to produce an antibody solution, which was added to assay-strip wells. After 90 min incubation at room temperature, DNA–protein samples were added to the wells that were pre-incubated with an anti-MYC or anti-IgG antibody. Precipitation of the DNA–protein complexes was performed overnight at 4 °C followed by intensive washing. Next, the samples were digested with RNAase and Proteinase K, after which DNA was purified using the column provided in the kit and analyzed by qPCR. The relative DNA amounts were calculated using the Fold Enrichment Calculation. The primers used to amplify the *PKP1* promoter were forward: 5´-CCA CCGGTTTTACAAGGCA-3´and reverse: 5´-GAAGAA AGTGGGGTAGGGGC-3´. Pre-immune IgG was used as negative control.

2.9 Site-directed mutagenesis of the *PKP1* promoter

MYC/MAX heterodimer recognition sites and MYC-MAX binding sites in the *PKP1* promoter sequence were detected using the online tool "MATinspertor" [16]. Site-directed mutagenesis was performed by PCR concatenation. We amplified the *PKP1* promoter from the "psiCHECK™-2-PKP1promoter" vector previously developed using the following primers: Shared cloning primer: BglII_FW_PKP1_PROM: ATATATAGATCT TGAGAAACCCAGGGCATCAAG, RV_PKP1_PROM_ NHEI: ATATATGCTAGCGGTGGCGGGAGGCGGGTG; PKP1 promoter Mut 1–2: Fw-promPKP1-mut1-up: GAA TAAAGCTTCACTGTCTAGATGTCCCCAGGGGTG , Rv-promPKP1-mut1-up: CACCCCTGGGGACATCTA GACAGTGAAGCTTTATTC, Fw-promPKP1-mut2-Dn: GGTTCCTGAGCTGAGTCTAGACTTTCTCAGTGAGC, Rv-promPKP1-mut2-Dn: GCTCACTGAGAAAGTCTA GACTCAGCTCAGGAACC; PKP1 promoter Mut 3: Rv-promPKP1-mut3-Dn: ATATATGCTAGCGGTGGCGGG AGGCGGGTGG TCTAGAGCCGGGGC.

The *PKP1* promoter was cloned upstream of the *Renilla* luciferase gene in a psiCHECK™-2 vector (Promega, C8021). We followed a conventional restriction enzyme cloning strategy with BglII and NheI. Firefly luciferase expression from the same bicistronic plasmid was used to normalize the transfection. Luciferase luminescence was determined using a Dual-Glo Luciferase Assay System (Promega, E2920) following the provided protocol.

2.10 Statistical analyses

The results are expressed as mean ± S.D. and represent at least two experiments. Statistical differences were analyzed using paired, two-tailed t-tests. Significance was considered when $p < 0.05$.

3 Results and discussion

To investigate the functional relationship between PKP1 and MYC in SqCLC primary tumors, we studied the correlation of their mRNA levels using a dataset we published previously (GSE18842) [9]. We found a significant positive correlation ($r = 0.62$, $p = 0.00018$) between the mRNA levels of *PKP1* and *MYC* in 31 SqCLC primary tumors (Fig. 1A). As a correlation control, *PKP1* mRNA levels were also tested against those of *TBP* (TATA-box binding protein), a common housekeeping gene. We corroborated our results using an independent dataset [17] of 73 SqCLC primary tumors (Fig. 1B).

Additionally, to confirm the value of PKP1 as a targetable biomarker, we determined the correlation between *MYC* and *PKP1* mRNA levels in lung squamous cell carcinoma (LUSC) and lung adenocarcinoma (LUAD) cohorts from The Cancer Genome Atlas (TCGA) [18]. We found that the *PKP1* and *MYC* mRNA expression levels were positively correlated in LUSC samples ($r = 0.26$, $p = 6.2\text{e-}09$), but not in normal tissue samples ($r = -0.002$, $p = 0.99$) or in LUAD samples ($r = 0.059$, $p = 0.18$) (Fig. 1C and D). Intriguingly, this correlation could not be explained by our previous observation that PKP1 enhances MYC protein levels while keeping *MYC* transcript levels unaltered [12].

Next, we tested whether the tumor-specific overexpression of *PKP1* and its correlation with *MYC* expression also holds in other squamous tumor types. With this aim, we analyzed data from TCGA-CESC (Cervix Squamous Cell Neoplasm), TCGA-HNSC (Head and Neck Squamous Cancer), and TCGA-ESCA (Esophageal Carcinoma). We found that all squamous tumors overexpressed *PKP1* compared to non-tumoral samples, and that this overexpression was strong in LUSC (FC = 51.7, $p = 2.2 \cdot 10^{-16}$) (Supplementary Fig. 1 and Supplementary Table 1). Conversely, we found that LUAD samples did not overexpress *PKP1* compared to normal samples ($p = 0.7$). In addition, we found that *PKP1* and *MYC* mRNA expression levels were correlated in the TCGA-CESC and TCGA-HNSC cohorts (Supplementary Fig. 2).

Having observed that the *PKP1* and *MYC* mRNA levels correlate in SqCLC primary tumors, we wondered whether MYC knockdown might affect the PKP1 levels. To test this, we selected several SqCLC cell lines that express PKP1 protein endogenously and transfected them with a siRNA

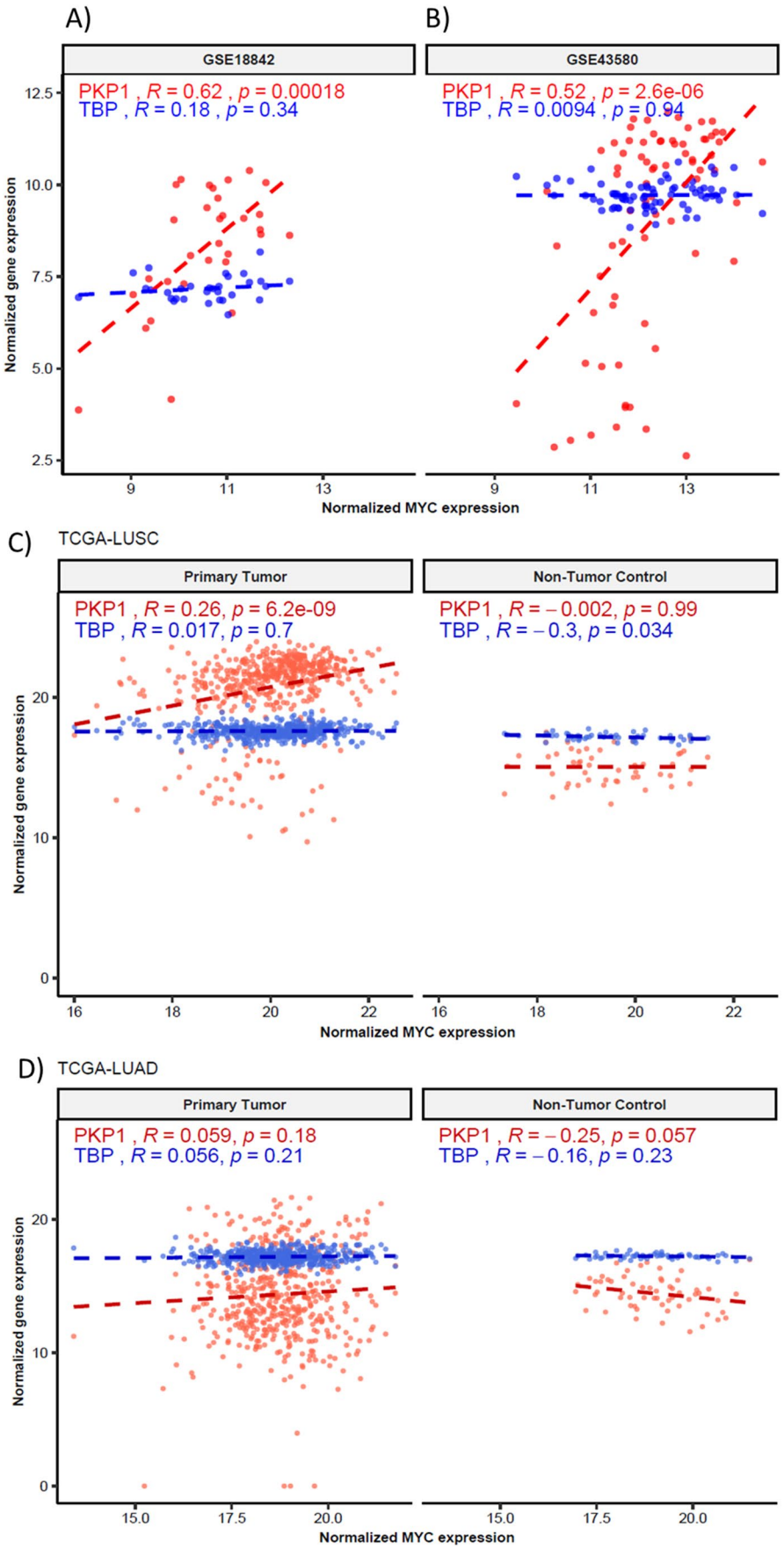

Fig. 1 **A** Correlation analysis of *PKP1* and *MYC* mRNA expression in SqCLC tumors in our previous study (GSE18842, $N=31$) [9] and **B** in an additional external study (GSE43580, $N=73$) [17], showing significant correlations between *MYC* and *PKP1*. The correlation between *PKP1* and *TBP* is included as a negative control. **C** Correlation analysis of *PKP1* and *MYC* mRNA expression from The Cancer Genome Atlas (TCGA) datasets TCGA-LUSC (Lung Squamous Carcinoma, $n=501$ primary tumors and 49 non-tumor controls) and **D** TCGA-LUAD (Lung Adenocarcinoma, $n=513$ primary tumors and 59 non-tumor controls). The correlation between *MYC* and *TBP* is included as a negative control. The Pearson correlation coefficient values (R), *p*-values and linear trends are shown. *PKP1*, plakophilin 1; *MYC*, MYC proto-oncogene; *TBP*, TATA-box binding protein

directed against MYC. As a control, we used scrambled siRNA under the same conditions. We assessed the PKP1 and MYC protein levels by Western blotting after 72 h of MYC inhibition. We found that the MYC knockdown was successful (~85% inhibition) and, interestingly, that it was followed by a consistent and significant reduction in PKP1 protein expression (~50% inhibition, $p=0.0003$) (Fig. 2A and B). This reduction in PKP1 was verified at the mRNA level by qRT-PCR ($p<0.05$) (Fig. 2C). These results suggest that PKP1 expression may be regulated by MYC.

On the other hand, we confirmed (as in our previous publication [12]) that PKP1 knockdown significantly reduced MYC protein expression (Fig. 2A) in three SqCLC cell line models: SK-MES-1, EPLC-272H and LUDLU-1 (mean fold change across the three cell lines = -1.5, $p=0.0001$). Furthermore, we previously found that PKP1 knockdown resulted in five MYC-related gene sets being inhibited [12], whereas PKP1 overexpression in two SqCLC cell lines (H520 and H2170) that do not express PKP1 endogenously resulted in increases in MYC protein levels (Fig. 2D).

To test whether MYC acts as a direct transcription factor for *PKP1*, we performed a chromatin immunoprecipitation (ChIP) assay targeted against MYC in SK-MES-1 cells. Presence of DNA from the *PKP1* promoter was checked by qPCR after MYC protein pulldown. We detected a significant direct interaction between MYC and the *PKP1* promoter (170% fold enrichment compared to the IgG negative control, $p=0.0079$) (Fig. 3A). To confirm a direct effect of MYC on *PKP1* transcription, we developed promoter-luciferase assays. To this end, we created bicistronic plasmids in which the *Renilla* luciferase gene is preceded by the *PKP1* promoter, and by which firefly luciferase is expressed to normalize the signal (Fig. 3B). We observed a significant decrease (over 50%, $p=0.0002$) in *Renilla* luciferase expression under the *PKP1* promoter after knocking down MYC using siRNAs (Fig. 3C). Next, using bioinformatic tools [16], we found three predicted MYC/MAX heterodimer binding sites in the *PKP1* promoter. To experimentally determine whether these predicted binding sites are functional, we created three different genetic constructs with mutations in the predicted MYC/MAX binding sites within the *PKP1* promoter (Fig. 3B). Subsequently, we measured changes in the luciferase signal after MYC or scrambled siRNA treatment. Interestingly, MYC knockdown reduced luciferase expression by ~60% in the construct with wild type PKP1 ($p=0.0002$) or the construct with mutations in the two predicted MYC/MAX binding sites furthest away from the transcription start site ($p=0.0001$). In contrast, we

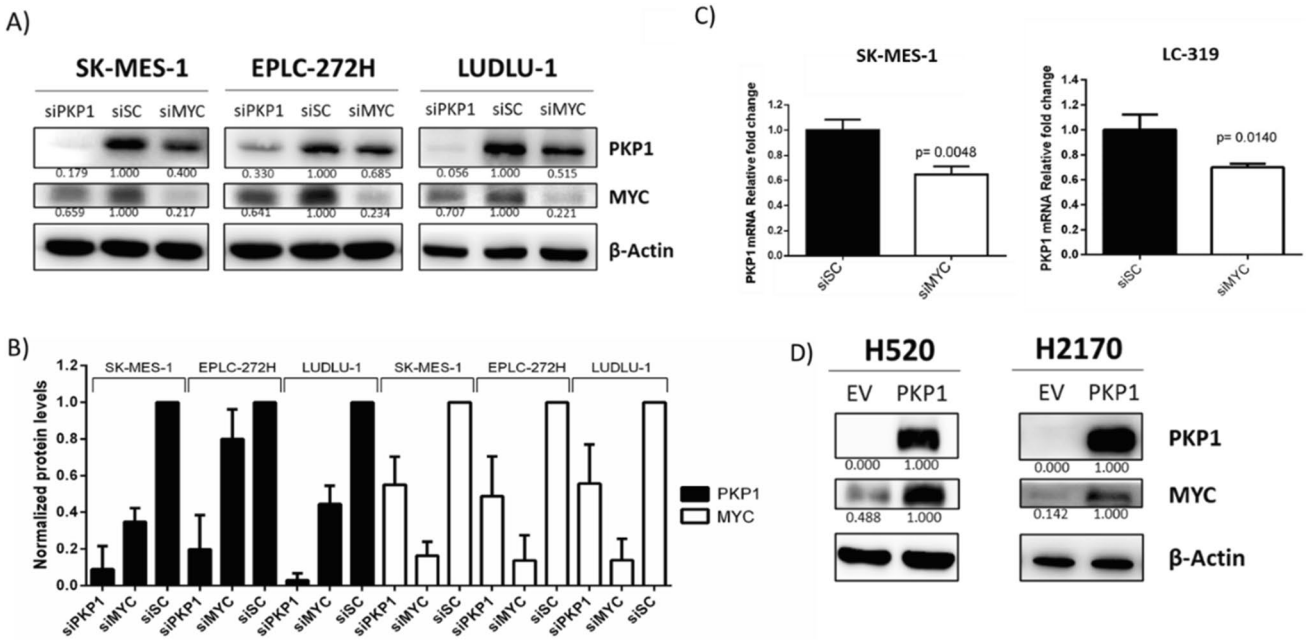

Fig. 2 **A** Representative Western blot assay of PKP1 and MYC protein expression after silencing of PKP1 or MYC in three SqCLC cell lines (SK-MES-1, EPLC-272H and LUDLU-1). Reduction in PKP1 or MYC induces their reciprocal inhibition. **B** Quantification of the PKP1 and MYC protein levels in response to PK P1 or MYC silencing, normalized against scrambled siRNA. The experiment was carried out in duplicate and β-actin was used as a loading control. **C** qPCR analysis of *PKP1* mRNA expression in SK-MES-1 and LC-319 cells after MYC silencing, showing that *PKP1* mRNA expression is significantly reduced by MYC inhibition ($p<0.05$). **D** Western blot assay of PKP1 and MYC protein status after exogenous PKP1 expression in SqCLC cell lines (H520 and H2170). Exogenous PKP1 expression induces MYC translation. PKP1, plakophilin 1; MYC, MYC proto-oncogene; β-Actin, anti-B-actin protein. siPKP1, knockdown siRNA against PKP1; siMYC, knockdown siRNA against MYC; siSC, scrambled-siRNA control

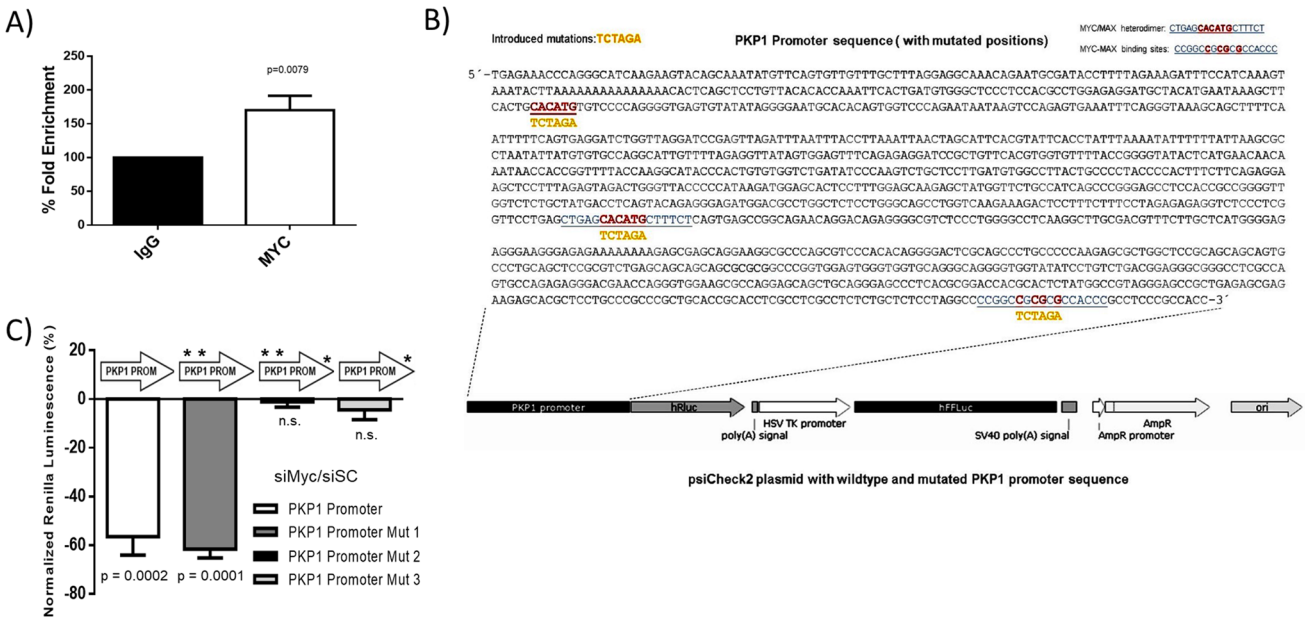

Fig. 3 **A** % Fold enrichment of *PKP1* promoter levels after chromatin immunoprecipitation (ChIP) of MYC protein. ChIP, chromatin immunoprecipitation; MYC, pulldown of *MYC*; IgG, pulldown of negative control. **B** Generated variants of the psiCheck2 plasmid. The plasmid is composed of two distinct promoters driving different luciferases. The *PKP1* promoter sequence was cloned just upstream of the *Renilla* luciferase gene, conditioning *Renilla* protein expression. Firefly luciferase gene expression was controlled by the *HSV-TK* promoter and firefly luciferase protein luminescence was used as normalizer. An altered sequence (in yellow) was introduced in the predicted MYC binding sites (in red). **C** Upper: psiCheck2 cloning strategy for *Firefly* luciferase assays on the *PKP1* promoter mutated (*) in different MYC binding sites. Lower: *Firefly* luciferase assay results showing a significant decrease in luciferase expression under the wild type *PKP1* promoter ($p=0.0002$) and the version with two mutated MYC/MAX heterodimer binding sites closest to the 5'-end of the *PKP1* promoter ($p=0.0001$) in the SK-MES-1 SqCLC cell line. On the other hand, the mutation of the MYC/MAX heterodimer binding site closest to the ATG start codon completely abolished the regulatory effect of MYC on the *PKP1* promoter compared to controls. *Firefly* luciferase expression in the same bicistronic psiCheck2 plasmid was used to normalize the signal. PKP1, plakophilin 1; MYC, MYC proto-oncogene. siMyc, knockdown siRNA against MYC; siSC, scrambled-siRNA control; PKP1 promoter Mut 1, psiCheck2 plasmid expressing 5´-end mutated version of the PKP1 promoter; PKP1 promoter Mut 2, psiCheck2 plasmid expressing 3´-end mutated version of the PKP1 promoter; PKP1 promoter, psiCheck2 plasmid expressing wild type PKP1 promoter; n.s., non-significant

found that the mutation in the predicted MYC binding site closest to the transcription start site led to complete resistance to the effects of MYC knockdown on PKP1 expression, thereby defining this binding site as the only functionally relevant one.

In this work, we have shown that MYC acts as a direct transcription factor of *PKP1* that binds to its promoter and regulates its expression. On the other hand, we previously reported that PKP1 enhances MYC translation [12]. Based on this bidirectional functional relationship between PKP1 and MYC, we propose a feedforward model in which PKP1 enhances MYC translation in conjunction with the translation initiation complex by binding to the 5'-UTR of *MYC* mRNA and, on the other hand, in which MYC promotes *PKP1* transcription by binding to its promoter. Interestingly, this mechanistic model, presented schematically in Fig. 4, could have relevant consequences for cancer therapy since it opens up the possibility to modulate MYC activity indirectly through PKP1.

Loss of desmosomes is a frequently occurring event in cancer and has been found to be related to invasiveness and metastasis [8, 19]. However, paradoxically, PKP1 (a primary component of desmosomes [20]) is recurrently overexpressed in SqCLC. Similar to other members of the armadillo family, PKP1 may have a context-dependent dual role, so that its oncogenic or tumor suppressive role is determined by its subcellular localization [5, 21]. This hypothesis is plausible since PKP1 has been found in the cytoplasm and in the nucleus, as well as in desmosomes [10]. Furthermore, based on its different subcellular localizations, different functions of PKP1 have been described, such as the promotion of cell growth [12], posttranscriptional regulation through mRNA ribonucleoprotein particles [22], translation and stabilization of attached mRNAs in stress granules [23], actin organization [20], DNA damage response by interaction with single-stranded DNA (ssDNA) [24], or regulation of translation dependent on the translation initiation factor eIF4A1 [25].

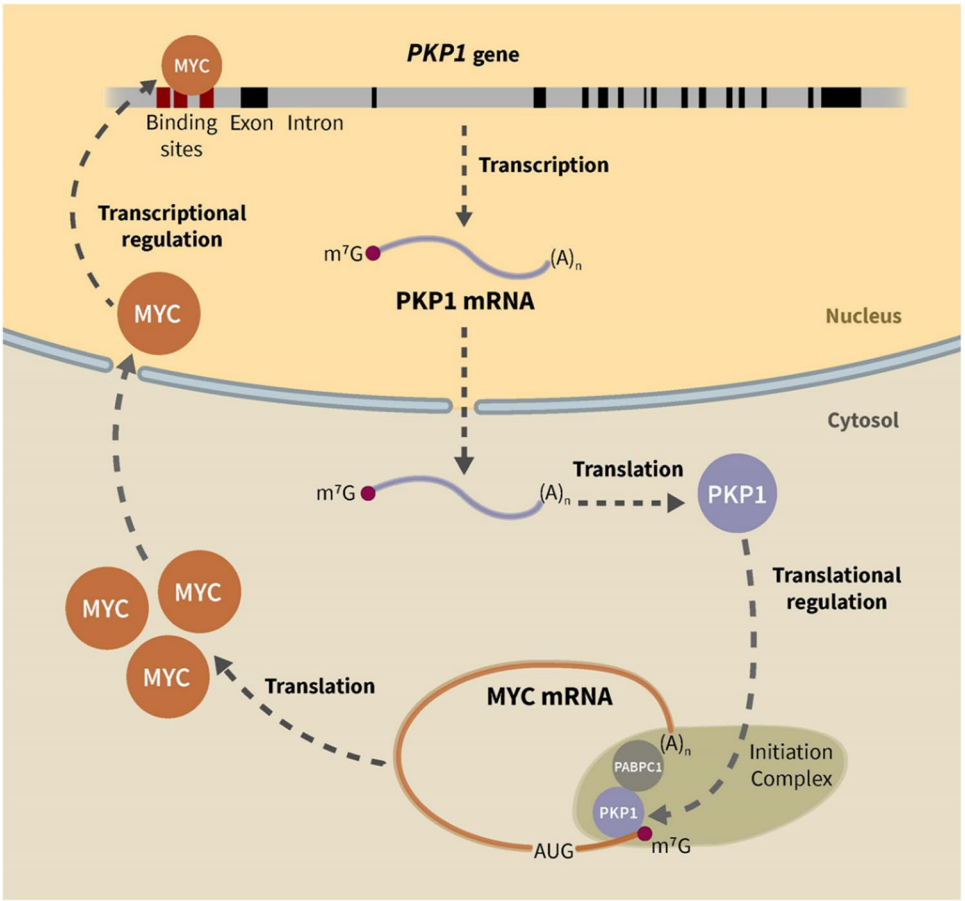

Fig. 4 Hypothesis of functional interaction between PKP1 and MYC at two levels: PKP1 as posttranscriptional activator of MYC; and MYC as transcription factor that directly binds to the *PKP1* promoter, enhancing its transcription. PKP1, plakophilin 1; MYC, MYC proto-oncogene; PABP, poly(A)-binding protein

In our study, we observed a strong positive correlation between *PKP1* and *MYC* mRNA expression in primary squamous lung tumors. This trend was also observed in other squamous tumors, but not in normal tissue or lung adenocarcinoma samples. This high specificity turns PKP1 into a good candidate biomarker for SqCLC and opens up new therapeutic opportunities for this histological cancer subtype. The data presented here, together with other recent findings of our group [12], suggest a mutual regulation of MYC and PKP1, forming a feedforward loop between both of them that links transcription and translation (Fig. 4). Such a loop operates at two levels. On the one hand, PKP1 acts as a posttranscriptional activator of MYC and, on the other hand, MYC acts as a transcription factor that directly binds to the *PKP1* promoter, thereby enhancing its transcription. Such a circuit may promote malignant cell transformation. Supporting our observations, other feedforward loops with implications for tumorigenesis have previously been described, linking MYC with other components of the translation machinery in other cellular models [26]. For example, altered signaling of the PI3K/AKT/mTOR pathway in cancer has bee n associated with changes in eIF4F transcription factor levels, thereby inducing alterations in the proteome that lead to expression of malignancy-related mRNAs such as *MYC*. Interestingly, very similar phenotypes have been observed when PKP1 or MYC were impaired in vivo [27, 28], reflecting our in vitro observations and supporting a feedforward loop interaction. Loss-of-function murine models of both genes have shown proliferation decrease, cell cycle arrest, apoptosis increase, growth retardation, developmental delay and a high perinatal mortality. The unveiling of this feedforward mechanism may pave the way for the development of new therapeutic strategies specific for SqCLC via indirect targeting of MYC. This could significantly improve the therapeutic options for SqCLC patients. SqCLC is heterogeneous in nature with a wide range of mutations without suitable targeted therapies, which severely limits current treatment options for these patients [29].

4 Conclusions

We found that MYC acts as a transcriptional regulator of PKP1 by directly interacting with the *PKP1* promoter and enhancing its transcription. This, together with previous results which indicate that PKP1 may act as a posttranscriptional regulator of MYC, establishes a feedforward loop not previously described. This functional relationship between

PKP1 and MYC suggests that inhibition of PKP1 may serve as a feasible indirect therapeutic approach to target MYC, a highly relevant oncogene that is currently "undruggable".

Supplementary Information The online version contains supplementary material available at https://doi.org/10.1007/s13402-022-00660-1.

Acknowledgements We acknowledge Ines Diaz for her technical support.

Author contributions L.B., J.M-P., M.I.R., P.P., F.R-S., A.M.A., and J.C. A.-P. performed and validated the experimental data. A.A. performed most of the bioinformatics and statistical analyses and reviewed and edited the manuscript. M.E. F-V. and M.C. provided supervision, expertise and feedback. L.B., P.P.M. and M.C. wrote the manuscript, analyzed and discussed the results. P.P.M. reviewed and edited the manuscript and provided conceptualization, validation, supervision, expertise and feedback, and participated in the funding acquisition and project administration.

Funding The CTS-993 group is funded by the Ministry of Economy of Spain (SAF2015-67919-R), the Junta de Andalucía (PI-0245-2017, PIGE-0440-2019, PI-0135-2020, PIGE-0213-2020, P20-00688), the Plan propio de la Universidad de Granada (PPJIA2019-06, and B-CTS-126-UGR18), an International Association for the Study of Lung Cancer (IASLC) Young Investigator Award 2017, and the Spanish Association for Cancer Research (LAB-AECC-2018). L.B, J.M-P, and D.J.G. were supported by a "Fundación Benéfica Anticáncer Santa Cándida y San Francisco Javier" predoctoral fellowship. L.B. is currently funded by the Ministry of Health and Social Welfare of Junta de Andalucía (RH-0051-2020). J.C.A.-P is a Marie Curie Postdoctoral Researcher (European Commission. H2020-MSCA-IF-2018 #837897). P.P. was supported by a PhD "La Caixa Foundation" LCF/BQ/DE15/10360019 Fellowship. A.A, A.M.A. and F.R-S were supported by a Spanish Ministry of Education, Culture and Sports FPU fellowship: FPU17/00067, FPU17/01258, and FPU19/05124.

Data availability The datasets generated during and/or analyzed during the current study are available in the Gene Expression Omnibus repository, https://www.ncbi.nlm.nih.gov/gds.

Declarations

Ethical approval and consent to participate This project has been approved by the institutional ethical committee of the University of Granada.

Consent of publication All authors of this manuscript approve its publication.

Competing interests The authors declare no potential conflicts of interest.

References

1. B. Angulo, A. Suarez-Gauthier, F. Lopez-Rios, P.P. Medina, E. Conde, M. Tang, G. Soler, A. Lopez-Encuentra, J.C. Cigudosa, M. Sanchez-Cespedes, Expression signatures in lung cancer reveal a profile for EGFR-mutant tumours and identify selective PIK3CA overexpression by gene amplification. J. Pathol. **214**, 347–356 (2008)
2. S.L. Topalian, F.S. Hodi, J.R. Brahmer, S.N. Gettinger, D.C. Smith, D.F. McDermott, J.D. Powderly, R.D. Carvajal, J.A. Sosman, M.B. Atkins, P.D. Leming, D.R. Spigel, S.J. Antonia, L. Horn, C.G. Drake, D.M. Pardoll, L. Chen, W.H. Sharfman, R.A. Anders, J.M. Taube, T.L. McMiller, H. Xu, A.J. Korman, M. Jure-Kunkel, S. Agrawal, D. McDonald, G.D. Kollia, A. Gupta, J.M. Wigginton, M. Sznol, Safety, activity, and immune correlates of anti-PD-1 antibody in cancer. N. Engl. J. Med. **366**, 2443–2454 (2012)
3. J.R. Brahmer, S.S. Tykodi, L.Q. Chow, W.J. Hwu, S.L. Topalian, P. Hwu, C.G. Drake, L.H. Camacho, J. Kauh, K. Odunsi, H.C. Pitot, O. Hamid, S. Bhatia, R. Martins, K. Eaton, S. Chen, T.M. Salay, S. Alaparthy, J.F. Grosso, A.J. Korman, S.M. Parker, S. Agrawal, S.M. Goldberg, D.M. Pardoll, A. Gupta, J.M. Wigginton, Safety and activity of anti–PD-L1 antibody in patients with advanced cancer. N. Engl. J. Med. **366**, 2455–2465 (2012)
4. D. Hanahan, R.A. Weinberg, Hallmarks of cancer: the next generation. Cell **144**, 646–674 (2011)
5. M. Hatzfeld, Plakophilins: multifunctional proteins or just regulators of desmosomal adhesion? Biochim. Biophys. Acta **1773**, 69–77 (2007)
6. J.A. McGrath, J.R. McMillan, C.S. Shemanko, S.K. Runswick, I.M. Leigh, E.B. Lane, D.R. Garrod, R.A. Eady, Mutations in the plakophilin 1 gene result in ectodermal dysplasia/skin fragility syndrome. Nat. Genet. **17**, 244 (1997)
7. E. Alatas, A. Kara, M. Kara, G. Dogan, O. Baysal, Ectodermal dysplasia-skin fragility syndrome with a new mutation. Indian J. Dermatol. Venereol. Leprol. **83**, 476–479 (2017)
8. R.L. Dusek, L.D. Attardi, Desmosomes: new perpetrators in tumour suppression. Nat. Rev. Cancer **11**, 317–323 (2011)
9. A. Sanchez-Palencia, M. Gomez-Morales, J.A. Gomez-Capilla, V. Pedraza, L. Boyero, R. Rosell, M.E. Fárez-Vidal, Gene expression profiling reveals novel biomarkers in nonsmall cell lung cancer. Int. J. Cancer **129**, 355–364 (2011)
10. M. Gómez-Morales, M. Cámara-Pulido, M.T. Miranda-León, A. Sánchez-Palencia, L. Boyero, J.A. Gómez-Capilla, M.E. Fárez-Vidal, Differential immunohistochemical localization of desmosomal plaque-related proteins in non-small-cell lung cancer. Histopathology **63**, 103–113 (2013)
11. T.N. Zamay, G.S. Zamay, O.S. Kolovskaya, R.A. Zukov, M.M. Petrova, A. Gargaun, M.V. Berezovski, A.S. Kichkailo, Current and prospective protein biomarkers of lung cancer. Cancers **9**, 155 (2017)
12. J. Martin-Padron, L. Boyero, M.I. Rodriguez, A. Andrades, I. Díaz-Cano, P. Peinado, C. Baliñas-Gavira, J.C. Alvarez-Perez, I.F. Coira, M.E. Fárez-Vidal, P.P. Medina, Plakophilin 1 enhances MYC translation, promoting squamous cell lung cancer. Oncogene **39**, 5479–5493 (2020)
13. Y.V. Svitkin, A. Pause, A. Haghighat, S. Pyronnet, G. Witherell, G.J. Belsham, N. Sonenberg, The requirement for eukaryotic initiation factor 4A (elF4A) in translation is in direct proportion to the degree of mRNA 5' secondary structure. RNA **7**, 382–394 (2001)
14. E.V. Schmidt, The role of c-myc in cellular growth control. Oncogene **18**, 2988–2996 (1999)
15. C.V. Dang, MYC on the path to cancer. Cell **149**, 22–35 (2012)
16. K. Cartharius, K. Frech, K. Grote, B. Klocke, M. Haltmeier, A. Klingenhoff, M. Frisch, M. Bayerlein, T. Werner, MatInspector and beyond: promoter analysis based on transcription factor binding sites. Bioinformatics **21**, 2933–2942 (2005)
17. A.L. Tarca, M. Lauria, M. Unger, E. Bilal, S. Boue, K. Kumar Dey, J. Hoeng, H. Koeppl, F. Martin, P. Meyer, P. Nandy, R. Norel, M. Peitsch, J.J. Rice, R. Romero, G. Stolovitzky, M. Talikka, Y. Xiang, C. Zechner, IMPROVER DSC Collaborators, Strengths and limitations of microarray-based phenotype

prediction: Lessons learned from the IMPROVER Diagnostic Signature Challenge. Bioinformatics **29**, 2892–2899 (2013)
18. The Cancer Genome Atlas Program - National Cancer Institute. https://www.cancer.gov/about-nci/organization/ccg/research/structural-genomics/tcga. Accessed 21 July 2021
19. S.T. Kundu, P. Gosavi, N. Khapare, R. Patel, A.S. Hosing, G.B. Maru, A. Ingle, J.A. Decaprio, S.N. Dalal, Plakophilin3 down-regulation leads to a decrease in cell adhesion and promotes metastasis. Int. J. Cancer **123**, 2303–2314 (2008)
20. M. Hatzfeld, C. Haffner, K. Schulze, U. Vinzens, The function of plakophilin 1 in desmosome assembly and actin filament organization. J. Cell Biol. **149**, 209–222 (2000)
21. A. Wolf, K. Rietscher, M. Glaß, S. Hüttelmaier, M. Schutkowski, C. Ihling, A. Sinz, A. Wingenfeld, A. Mun, M. Hatzfeld, Insulin signaling via Akt2 switches plakophilin 1 function from stabilizing cell adhesion to promoting cell proliferation. J. Cell Sci. **126**, 1832–1844 (2013)
22. R. Fischer-Kešo, S. Breuninger, S. Hofmann, M. Henn, T. Röhrig, P. Ströbel, G. Stoecklin, I. Hofmann, Plakophilins 1 and 3 bind to FXR1 and thereby influence the mRNA stability of desmosomal proteins. Mol. Cell. Biol. **34**, 4244–4256 (2014)
23. I. Hofmann, M. Casella, M. Schnölzer, T. Schlechter, H. Spring, W.W. Franke, Identification of the junctional plaque protein plakophilin 3 in cytoplasmic particles containing RNA-binding proteins and the recruitment of plakophilins 1 and 3 to stress granules. Mol. Biol. Cell **17**, 1388–1398 (2006)
24. T. Sobolik-Delmaire, R. Reddy, A. Pashaj, B.J. Roberts, J.K. Wahl 3rd., Plakophilin-1 localizes to the nucleus and interacts with single-stranded DNA. J. Invest. Dermatol. **130**, 2638–2646 (2010)
25. A. Wolf, M. Krause-Gruszczynska, O. Birkenmeier, A. Ostareck-Lederer, S. Hüttelmaier, M. Hatzfeld, Plakophilin 1 stimulates translation by promoting eIF4A1 activity. J. Cell. Biol. **188**, 463–471 (2010)
26. C.J. Lin, A. Malina, J. Pelletier, c-Myc and eIF4F constitute a feedforward loop that regulates cell growth: implications for anticancer therapy. Cancer Res. **69**, 7491–7494 (2009)
27. M. Pirity, J.K. Blanck, N. Schreiber-Agus, Lessons learned from Myc/Max/Mad knockout mice. Curr. Top. Microbiol. Immunol. **302**, 205–234 (2006)
28. K. Rietscher, A. Wolf, G. Hause, A. Rother, R. Keil, T.M. Magin, M. Glass, C.M. Niessen, M. Hatzfeld, Growth retardation, loss of desmosomal adhesion, and impaired tight junction function identify a unique role of plakophilin 1 in vivo. J. Invest. Dermatol. **136**, 1471–1478 (2016)
29. E.S. Santos, L. Hart, Advanced squamous cell carcinoma of the lung: current treatment approaches and the role of afatinib. Onco. Targets. Ther. **13**, 9305–9321 (2020)